Mobilisation Features and Environmental

Mobility of Gold across New Zealand

Lachlan Stewart[1]

[1]. University of Adelaide, Honours program 2010

Supervisor: Frank Reith

27/11/10

Contents:

1. **Abstract:**

Gold from localities across New Zealand; including Southland, Central Otago, the West Coast, and the South Coast, were studied using scanning electron microscopy. Sites were chosen based on contrasting relationships of environments to compare and contrast the fine micrometer and nanometer scale features present on the gold. Using the latest equipment for subsurface imaging, that included a focused ion beam scanning electron microscope, gold mobilisation features were indentified. Features include gold precipitation and aggregation structures, dissolution and fluvial transport damage, as well as nano-particulate formation seen on samples from every site. Secondary features are present on all of the sampled gold grains and are the result of remobilisation, aggregation and dispersion of the samples while in the supergene environment and not the result of prior processes. Nano-particulate dispersion is discussed as the possible source for gold precipitation and aggregation due to its high reactivity and gold's natural affinity towards itself. Nano-particulates are also identified as the gold form resulting from the etching of underlying gold and the principle feature by which gold nano-particulates are created and subsequently dispersed.

2. **Introduction:**

Gold has been highly sought after for its precious metal value since the beginning of recorded history, and has served as a symbol of wealth and as a store of value throughout. Its attractive properties, symbol of wealth and electrical properties have increased its uses in today's world from jewellery to electrical contacts and cables, especially in computers, as well as the latest

medicines, despite the decline of its use in maintaining and trading of money by coins and bars. Fundamental to maintaining the uses of gold relies on maintaining a steady supply through understanding its characteristics, physical processes, and chemical behaviour both below the ground and in the environment, mineralisation styles and formation of deposits of economic value which can be thought of as the gold cycle. The gold cycle begins with the formation of deep sulphide hosting gold containing system, this can also occur as a sub surface hydrothermal system, which may or may not be derived from the dissolution of gold from deep sulphide bodies. The deposition of gold in primary deposits usually occurs via metal rich hydrothermal fluids, which circulate in open spaces within rocks and deposit gold as a consequence of cooling or boiling (Morteani, 1999). At the Earth's surface the gold containing rocks and minerals undergo erosion processes leading to the release of free gold or gold containing alloys into the environment. Two conflicting theories have been proposed since the major gold rushes of the 1800's as to the behaviour of gold in the environment; one is the detrital theory most recently supported by Hough (2007) and the other is accreationary theory most recently supported by Reith (2007). Detrital theory is currently applied to gold nuggets usually weighing greater than 1gram, having been formed by physical processes of movement and de-alloying of silver in alluvial environments, originating from primary deposits. These nuggets are characterised by a depleted outer rim and an alloyed core containing silver and or mercury and are generally referred to as primary gold. Accreationary theory is generally applied to gold weighing less than 1 gram and is generally exceedingly pure (>99%) gold. This theory is based on the solubilisation of gold, as gold complexes and the movement through the environment until the complex is either destabilised due to a change in the chemical conditions, resulting in the precipitation of the gold, or by the bacterial interaction on the gold containing complexes also resulting in the precipitation of the gold. Gold precipitated by chemical or biological means is generally termed secondary gold, which can also occur on the surfaces of primary gold through the local solubilisation and re-precipitation of the

underlying gold. Fine particles of secondary and bacterioform gold can also be released into the environment as highly reactive particles that are cable of promoting further concentration; such as soils, calcrete and placers or growth of gold grains through aggregation (Lengke, 2007; Reith, 2010). Physical processes have the greatest influence on the concentration of primary gold, forming alluvial gold systems, such as those in the Victorian goldfields of Australia, while geochemical and geological conditions have the greatest influence on the concentration of secondary gold. Secondary gold systems include quartz pebble conglomerate (QPC) style systems, such as the great Witwatersrand Basin in South Africa and the Waimumu district in Southland, New Zealand. Quartz pebble conglomerate systems are the result of recycling of conglomerates and the redeposition of quartz rich (greater than 80 vol% quartz) gravels. The processes of gold enrichment in the Archean QPC systems is still debated, due to the influence that low metamorphic processes had on the gold morphologies or whether the morphologies are the influence of surface condition, chemical and or biological processes. A previous study by Reith (2010), was aimed at the characterisation of some naturally occurring gold morphologies from Queensland Australia, with particular attention to the secondary gold structures. Reith et al. Demonstrated that (i) microbially-driven dissolution, precipitation and aggregation leads to the formation of bacterioform gold, and contributes to the growth of gold grains under supergene conditions; and (ii) the microbially driven remobilisation of coarse gold into nano-particulates plays a key role in mediating the mobility of gold in Earth's surface environments, because the release of nano-particulate gold upon biofilm disintegration greatly enhances environmental mobility compared to gold-complexes. Research and laboratory studies have showed cyanobacteria, sulphide-oxidising, and metallophilic, as well as sulfate-reducing bacteria biomineralise nano-particulate gold from gold (1/III) complexes (Lengke, 2006b; Lengke, 2006a; Lengke, 2005; Lengke, 2007), and in their presence aggregate, transforming into gold octahedral crystals within weeks(Southam, 1994; Southam, 1996) and evolving over several months into coiled or wire gold with irregular and

rounded structures that are morphologically similar to bacterioform gold (Lengke, 2007). Gold grains and or nuggets between 0.1 and 4mm in diameter are the most abundant source of alluvial and eluvial gold in the supergene environment and constitute economic important deposits such as the Witwatersrand deposit (Mossman, 1999). Falconer (2003) conducted research on a QPC gold deposit in Southland, New Zealand, with the aim of comparing observed morphologies of gold and sulphide minerals of an unmetamorphosed QPC with those structures and morphologies observed on the Archean, low metamorphosed QPC's of the Witwatersrand Basin deposit. This study allowed for a better understanding of pre-metamorphism formation of the QPC system with post depositional sulphide mineralisation in the surficial environment despite the oxygen-rich atmosphere. The textures described by Falconer (2003) are often prescribed to the metamorphic influence on the gold and sulphides of the Witwatersrand Basin, despite the unmetamorphosed state of the New Zealand QPC's.

Falconer (2003) study was looking to classify and compare observed structures of the gold and sulphides with those of the Witwatersrand and other Archean deposits, while Reith (2010) was classifying textures with specific attention to the biological influence and processes related to those gold grains. This study aims to use both studies to understand the mechanisms of gold transport across a range of gold systems in New Zealand; from the eluvial QPC deposits of Southland, New Zealand; focussing on secondary gold structures and possible mechanisms of formation, to the alluvial gold fields of the West Coast of New Zealand; comparing features and morphologies, and finally the beach placer deposits of the South Coast of New Zealand also comparing features. This study will be specific to New Zealand gold with an adjunct of 1 South Australian gold system, as New Zealand has current active and recent gold concentration systems, with the currently forming geology and processes of New Zealand. The importance of this can be represented by a comparison with the continent of Australia and its gold deposits and systems, which are often ten to hundreds of millions of years old and the rather arid climate of Australia. Climate and active geology are

important related back to the influence each have on the chemical system of the surface environment, which has a direct influence on the concentration of secondary gold systems and processes. Climate can be related to the state of vegetation which are capable of releasing organic components into the environment that are capable of complexing, transporting and depositing gold chemically (Reith, 2007). Mean temperature can also have an influence when related to the formation of peat and lignite capable of forming sulphide mineralisation and reductive gold precipitation (Falconer, 2003). Understanding secondary gold systems and the mechanisms of gold transport in the supergene environment increase the understanding of metal mobility, not only gold, within the surface environment and improve exploration for economically significant secondary gold deposits such as the QPC systems of New Zealand and South Africa, which would be characterised by searching for specific geochemical, climatic, and potentially biological features of these deposits.

3. Site Description:

Sites were chosen to have the best contrasting effect when looking at their particular methods of formation and concentration. The main site for study was the same site as previous research conducted by Falconer (2003), at a road aggregate quarry known as Parker Road, Waimumu, Southland, New Zealand (GPS; UTM 59G, 0329879, 4889413). This was chosen to undertake further research using the latest equipment to better identify any structures on the gold grains, which may be due to secondary formation processes. The geology here is inclined to the formation of secondary gold, where underlying gore lignite measures have been recycled to form the current QPC gold bearing systems (Falconer, 2003); classing this system as eluvial due to the localised recycling/redeposition of the QPC (Waimumu gravels). Climate here is quite different from some of the other study sites, such as those on New Zealand's west coast; with a mean annual rainfall of 918mm and a mean annual temperature of $9.7^{\circ}C$ (Falconer, 2003).

Central Otago, South Island, New Zealand was sampled and studied to compare the observed features with those of Parker Road; whose gold source is believed to be from this area (Falconer, 2003). 2 sites here included Kawarau gorge and Arrow Town (GPS; UTM 59G, 0330998, 5015601) located only a small distance apart (fig. 1). Climate is similar to the Parker Road site with a mean annual rainfall of 913mm, and a mean annual temperature of 11.5^{o}C. These sites are characterised as alluvial systems with the gold being sampled from active stream placers and stream gravel deposits, for Arrow Town and Kawarau gorge respectively.

Contrasting to the climate of the central and lower South Island of New Zealand is the gold systems of the west coast. Gold from here was sampled from Shanty Town (GPS; UTM 59G, 0514816, 5290335) in a placer style gravel deposit, and store bought samples from Reefton (GPS; UTM 59G, 0571347, 5337064) to the north believed to be local samples. These sites were chosen due to the vastly different climate of the west coast receiving an annual rainfall of 2875mm and a mean annual temperature of 14°C; subsequent to this is the high level of vegetation on the west coast, which could provide chemical systems for the mobilisation and movement of gold.

The final site was chosen also because of the contrasting climate, and the results of a previous study by McCann (2009), which is on the South Coast of the South Island, New Zealand (GPS; UTM 58G, 0710281, 4871426). Annual rainfall here is 1112mm with an annual average temperature of 10°C, however, the important point here is the effect of frequent storm surges, wind and salt water erosion have on the mechanisms and concentration of the gold, and the subsequent morphologies they record.

3.1 Parker Road

Parker Road lies within the Waimumu area (Fig. 1a) of Southland, New Zealand. Basement is comprised of the Murihiki terrane greywacke, overlain by Oligocene marine sedimentary rocks,

and Tertiary non-marine strata; which are dominated by the Gore Lignite Measures (Isaac, 1990). Uplift during the Cenozoic has resulted in the recycling of the Tertiary non-marine conglomerates, which lead to the redeposition of the Waimumu QPC. The site at Parker Road has at least 3 stratigraphic horizons including a thin carbonaceous mudstone which overlays the, at least, 10 meter thick QPC and the Gore lignite measures, which, were discovered on the day of sampling, presumably offset by the adjacent Hedgehope fault; with gold occurring in all 3 sequences at Parker Road. The QPC at Parker road has been sporadically mined as a source of road building aggregate (Falconer et al., 2006), and now also includes a gold recovery operation.

3.2 Kawarau gorge

The Otago Schist belt to the North has numerous mesothermal vein systems (Craw, 1991), which have shed gold leading to the formation of gold placers throughout Otago and Southland (Falconer et al., 2006). Gold was sampled in Central Otago as a comparison to that of the Waimumu gold grains, at a tourist gold centre in the Kawarau gorge (Fig 1b). The sampling material was locally derived conglomerates of up to pebble sized gravels.

3.3 Arrowtown

The gold sampled in the Kawarau gorge is in close proximity to the next sample site at Arrowtown, New Zealand (fig. 1b), in which gold bearing stream gravels were sampled.

3.4 Shanty Town

Shanty Town, New Zealand (Fig. 1c) is a recreated town based on a 19th century "gold rush" style. Conglomerate gold bearing gravels are hydraulically sluiced using a long tom set-up; a long channel with bars perpendicular to the channel and water flow, which gold is separated

gravimetrically by its density. Uplift along the Southern Alps has formed hydrothermal vein hosting gold mineralisation and weathering on both sides of the Alps, including glacial periods and effects, leads to the formation of gold placer deposits in current streams and rivers (Koons, 1990). Shanty Town lies to the west of the Alpine fault 10km south of Greymouth, New Zealand, alongside Infants Creek, possibly a source for the local gold placer, despite no available research papers.

3.5 Reefton

Gold grains were obtained from a shop in Reefton (Fig. 1c) with the assurance of the store owner that they were samples local to the area.

3.6 Orepuki Beach

The site referred to, in this paper as Beach Placer, comes from a location on the coastline east of Orepuki, New Zealand (Fig. 1d). This site was also the same as a previous study by (McCann, 2009); site 8/9. This site rests on a fragment of Palaeozoic Gondwana; consisting of granitic rocks, Devonian to Carboniferous, intruding metasedimentary rocks of the lower Palaeozoic age. McCann (2009) summarises that the erosion of the eastern Fiordland granites supply the majority of sands and gravels which are deposited along the beaches of the south coast. The climate of the south coast has the largest influence on the deposition and formation of heavy mineral leads on the beaches; with calm weather tides bringing up the heavy mineral leads, which form these placer deposits. The south coast is prone to storm surges of the south Pacific and the rough weather that is common in the Foveaux Strait; which has a large influence on the beach structure and of the metals in the heavy mineral leads. At Orepuki the high tides and storm surges wash over and remove the dunes, with high winds influencing saltation, dune size and erosion on the coast (McCann, 2009).

3.7 Echunga

Gold grains were also obtained from a location local to the author at Echunga, South Australia (Fig. 1E). These were added as an addendum to the main research, to further analyse any possible structures. Echunga was the site of a gold rush during the 1860s, with the gold occurring in palaeo-channel deposits of Tertiary age, the main stratigraphic unit consisting of Torrensian sediments, of the Adelaide fold belt. The conglomerates consist of quartz and iron-oxides, with the heavy mineral portion consisting of garnet fragments, iron oxides and fine zircon sand.

4. Methods:

Gold grains from the sites of Parker Road, Central Otago, Arrowtown, Shanty Town and the Orepuki Beach Placer; were sampled according to a specific procedure aimed at stabilising and preserving any and all structures present on the gold grains. All equipment was field sterilised with methylated spirits prior to sampling and care was taken to prevent cross contamination of sample sites. Two of the horizons at Parker road were sampled by panning material from the sieve processing plant (QPC) and from direct outcrop of the Gore lignite measures, with several sterile gold pans of heavy mineral concentrate collected. Concentrate and individual sampled gold grains were washed with sterile saline solution, and then stored under saline and transported as cold as possible returning to the laboratory. Gold grains from Reefton were stated not to have been treated in any way prior to purchase, or prior to being studied. Samples from Shanty Town were gathered from the first riffle or bar perpendicular to the water flow, in the Long Tom channel, after 30 minutes of hydraulic sluicing had taken place, and then sampled according to the process aimed at stabilising and preserving structures. Echunga gold samples were panned with no regard to sterile conditions and were transported and stored dry at room temperature, in sealed tubes. Prior to analysis, the gold grains were separated from concentrate using sterile equipment and washed

several times with distilled, deionised water to remove salt, and then air dried. Four samples from each site were mounted on adhesive tape, using a fine paintbrush under a stereomicroscope, fixed to sample holders and analysed initially, uncoated, using field emission scanning electron microscopy (FEG-SEM, Philips XL-30, Adelaide Microscopy, Australia). Parker Road and Shanty Town sample holders were then coated with an unknown thickness of carbon film and studied using a focussed ion beam-scanning electron microscope (Fib-SEM, Helios NanoLab Dual Beam, Adelaide Microscopy, Australia). When the site on the grain to be studied was located it was locally platinum coated at $2pA/um^2$ (Fig. 2A), to preserve "soft" surface features which might otherwise be damaged during cutting. Sections were then cut using a FIB at 30KeV and 21nA or 9.2nA (Fig. 2B); using a lower current for a smaller cutting area, then successively cleaned by reducing the beam current to 30KeV at 2.7nA and finally to 30KeV at 0.21nA (Fig. 2C). Microprobe analyses were conducted by imbedding samples in vacuum cured epoxy resin, using sandpaper to successive finer grades and polishing with up to 1um diamond paste and then carbon coating. The composition of Au, Ag, Fe, and Hg was quantitatively mapped by wavelength dispersive x-ray (WDX) using a Cameca SX51 microprobe (Adelaide Microscopy, Adelaide), that had been preset to the desired metal standards prior to analysis. Other elements including; Fe (0.07%), Ni (0.09%), Cu (0.11%), Zn (0.13%), As (0.27%), Pd (0.25%), Sn (0.18%), Os (0.34%), Ir (0.36%), Pt (0.48%), Hg (0.62%), Pb (0.40%), Al (0.06%), S (0.06%), Bi (0.53%), and Sb (0.17%) were included and quantified while only As, S, Cu, Sn, Pt, Pd, Pb and zinc were mapped using the energy dispersive x-ray spectroscopy (EDXS).

5. Results:

5.1 Parker Road QPC

Gold grains studied from the Parker Road QPC are all fine grained gold; between 100 and 1mm in length (Fig. 3A). The fine grained gold is flattened, sub rounded to rounded platy grains

with prominent folded edges, flat surfaces and numerous cavities. The grain edges are between 10 and 20um thick, have rounded and sometimes thickened edges developing to folds and can have sharp angular tears propagating into the gold grain from the edge up to 100um. The surface of the gold is mostly flat and smooth (Fig. 3B), with carved channels containing prominent striations representing slicken slides. They have numerous inclusions of either aluminosilicate or silica in the form of quartz; and are often deep under the surface or are covered by thin branched networks of gold (Fig. 3C). The gold grain contains cavities spread across all surfaces; some can be up to 20um wide which contain and protect crystalline and microcrystalline gold from damage; particularly when located close to folded rims. Gold within the cavities is often in the form of flat step like gold sheets, or of a porous branched network style which may include fine particles of aluminosilicate, and or free nano-particulate gold. Both the flat stepped gold sheets and porous branched networks of gold can have highly developed valleys between what appear as individual gold crystals, or dissolution textures, which exposes the crystal boundary of individual gold particles (Fig. 3D), and yet other areas display no or very little development of dissolution boundaries (Fig. 3C). The porous branched networks of gold display a tendency of occurring over silica inclusions within the gold grain. This feature appears as though the gold is overgrowing the inclusion (Fig. 3C), and yet also display some crystal boundary dissolution giving these features a budding style bridge appearance across the silica. Element maps across the grain interiors show, moderately developed, higher purity, gold rims and a subsequent higher concentration of silver in the interior of the grain. The silver concentration within the grain core can be as high as 11.12% Ag and an average of 7.64% Ag across the entire grain (Fig. 3F), while grain rims have silver which is typically below detection limit of 0.26% Ag. Gold concentration on the rim of the grain can be as high as 100% Au, while the grain core at the highest silver concentration is also the lowest gold concentration of 90.63% Au (Fig. 3E), with the gold / silver ratio appearing generally inversely proportional. The average gold concentration across the entire grain is 92.8% Au. Trace

elements were also analysed, yet only Si had a concentration above detection limit of a max 37.6% Si, possibly due to a silica inclusion in the polished block as this spot had 2.30% Au concentration, average Si concentration was 0.06% Si and detection limit of 0.057% Si. Elements below detection limit included Fe, Ni, Cu, Zn, As, Pd, Sn, Os, Ir, Pt, Hg, Pb, Al, S, Bi, and Sb, noting that these gold grains did not contain any detectable mercury, which may have an influence on gold structures. Fib analyses in a topographically low region, and thus protected from damage striations, provided a 3D representation of below surface structures (Fig. S2). The subsurface milling displays a prominent cavity filled polymorphic surface layer, containing inclusions of silica, below which, is at least a 20um thick region of fine microcrystalline gold (Fig. 4B, C). On the lower left hand side of the subsurface face, about 20um below the surface is a large cavity or silica inclusion up to 5um deep by 20um wide (Fig. 4C). The movie (Fig. S2) displays this feature with an enlarging rolling motion further into the face. Concurrently with this motion is the reduction in size of a region of coarse crystalline gold, being replaced by the microcrystalline gold not in the same crystal orientation (Fig. S2, 6-11seconds). The microcrystalline gold appears as relatively similar in crystal orientation and a maximum of 5um in length and 3-5um in depth. This band also has a detectably higher concentration of Ag, by an element map (Fig. 4D), despite not being quantified. The band between 5um in depth to 20um in depth displays this feature and does not progress any deeper into the grain and remains in the region of the smallest grain size microcrystalline gold; maximum of 5um in length and 1um in depth.

5.2 Parker Road Gore Lignite Measures

The gold sampled from the Gore Lignite horizon at Parker Road displays many similar characteristics of the QPC. The gold is fine grained 300 - 1000um in length, sub rounded to rounded, flattened platy grains, with prominent folded edges, flat surfaces and numerous cavities (Fig. 5A, B). The grain edges are between 10 – 20um thick, rounded, flat and some grains have

numerous tears propagating up to 200um into the grain. Two of the sampled grains are covered by a significantly textured surface, with very little or no carved channels containing striations, one sampled grain is covered by a moderately flat, smooth surface also lacking in striated carved channels, and the other sampled grained has a moderately textured surface containing numerous carved striated channels. The predominant gold structure on the textured grains is due to extensive networks of branched gold, while smooth flat grain surfaces are due to stepped flat sheets of gold with all gold samples showing inclusions of silica and aluminosilicates. Samples with textured surfaces contain many cavities (Fig. 5C) protecting fine branched filaments; including those over silica inclusions which appear as overgrowths (Fig. 5E), and nano-particulates (Fig. 5D). These samples preserve less fine etched valleys of grain boundary dissolution but where they do occur can be moderately developed creating a budding style texture (Fig. 5E). Element maps across grain interiors show poorly developed gold enriched rims, however, record higher concentrations of Ag within grain cores. Silver in the grain core can reach as high as 8.57 % Ag, with grain rims typically below the detection limit of silver 0.26% Ag. Average silver concentration across the grain interiors varies between 1.41% Ag and 2.04% Ag. The gradient of silver concentration across the grain is sharply defined in one sample; with the silver isolated to 2 small distinct regions of high concentration of silver (Fig. 5I), and disseminated in another sample (Fig. 5G); with a moderate concentration of silver spread across the grain. Gold concentration can be as high as 100% Au with very high consistent gold values averaging 97.4 % Au (Fig. 5F and H) with a standard deviation of only 2.09. The only other detected element present was silica; with a maximum concentration 0.28 % Si on the edge of the grain, with an average value across the grain of 0.069 % Si and detection limit of 0.057% Si. Elements below detection limit included Fe, Ni, Cu, Zn, As, Pd, Sn, Os, Ir, Pt, Hg, Pb, Al, S, Bi, and Sb, noting that these gold grains did not contain any detectable mercury, which may have an influence on gold structures.

5.3 Shanty Town

The grains sampled from Shanty Town present a very complex surface structure comprised of a highly textured surface with many carved striated channels, topographic lows, which have not progressed into cavities, long thin networks of carbon based (EDAX spot analyses) organic like material, many inclusions of silica, aluminosilicate and some iron titanium oxides and vast regions of nano-particulate gold up to and exceeding 100um in width. The sampled grains are between 200 and 800 um in length, sub rounded to rounded (Fig. 6A), flattened platy grains, with some folded re-flattened edges, highly textured surfaces and some cavities. The grain edges are smooth, rounded and 10-50um in thickness. One of the sampled grains surface is highly texture and is comprised of extensive branched networks of gold and flat step like gold sheets. The surface contains carved striated channels, topographic lows; which preserve the fragile gold forms, and some cavities that contain crystalline silica (Fig. 6F). The other sampled grain contains folded re-flattened edges, an intensely damaged surface with many carved striations, topographic lows containing vast regions of nano-particulate gold (Fig. 6C) and a network of thin carbon based (EDAX spot analyses), organic like material (Fig. 6B, D and E). The networks of carbon based material can occur near to (within 20um) the regions of nano-particulate gold, and maybe have some correlation. The highly textured surface of both samples traps and contains many inclusions of silica, aluminosilicates and rare iron titanium oxides. The samples have low to highly developed valleys between individual gold crystals representing grain boundary dissolution, and have in rare cases isolated individual gold crystals from the bulk material. Element maps across the grain interior show poorly developed silver depletion rims, which are only identified by quantification transect across the grain. Silver concentration (Fig. 6H) in the grain interior is a maximum of 2.34% Ag, with the grain edges often recording no value for Ag by quantification with a detection limit of 0.27% Ag, while average silver concentration across the grain is 1.51% Ag. An isolated quantitative spot analysis of silver concentration returned a value of 36.7% Ag, which was not

recorded across the transect. Gold concentration (Fig. 6G) can be as high as 100% Au on the grain edge, while grain interiors have a minimum gold concentration 98.30% Au and average gold concentration across the grain 99.44% Au. The instrument detection limit for gold was 0.28% Au. The only other element which recorded a value was silica, despite being often close to the detection limit of 0.05% Si, a maximum value of 1.51% Si was recorded on the samples edge with an average across the grain of 0.17% Si. Elements below detection limit included Fe, Ni, Cu, Zn, As, Pd, Sn, Os, Ir, Pt, Hg, Pb, Al, S, Bi, and Sb, noting that these gold grains did not contain any detectable mercury, which may have an influence on gold structures. Fib analyses yielded a complex polymorphic and below the gold surface structure, including a polymorphic layer containing microcrystalline gold (Fig. 7C, E), areas of coarse crystalline and microcrystalline gold in the subsurface extending to depth (Fig. 7B), long thin bands (some <0.5um deep) of microcrystalline gold (Fig. 7D), indistinct crystalline boundaries on gold crystals as well as highly distinct boundaries on coarse crystalline gold and a second polymorphic layer beginning at 30um extending deeper into the sample (Fig. 7A). The polymorphic layer on the surface of the gold is approximately 30um wide by 8 um deep, and contains numerous microcrystalline gold forms (some as small as 10nm wide) which preserve crystalline orientations and boundaries within them (Fig 7E). At the interaction between the polymorphic layer and the gold surface numerous pits etched into the gold surface are displayed, some 3um deep, filled by the polymorphic material (Fig 7C). Below the polymorphic layer gold occurs as both microcrystalline and coarse crystalline gold. Coarse crystalline gold is only present just below the surface with no regions of it extending to depth and displays a number of crystal orientations with sharp distinct boundaries. The bulk of the subsurface makeup is that of fine microcrystalline gold occurring with indistinct crystal boundaries, non linear, crystalline orientations and long, elongated, thin bands. The long, elongated bands are orientated roughly horizontally with respect to the sample surface, dipping to the right of the section into depth. They display a mylonitic style texture, in which the bands are

comprised of roughly parallel horizontally aligned micro-crystals (Fig 7A, D), which are of finer grain size than the bulk of the subsurface. The bands do not appear to affect the crystal orientations either side of the mylonitic zone, with the microcrystalline orientations remaining continuous on either side. The microcrystalline gold in the top 30um of the surface display indistinct crystalline boundaries; some appearing almost radially orientated, while deeper they become sharper, and of slightly larger grain size (3-5um). The second polymorphic region starting at 30um and extending to depth shows similar features as the surface layer and an observed width of 40um.

5.4 Kawarau gorge

The sampled gold grains from the tourist gold centre in Kawarau gorge, Central Otago, is fine grained 500-1000um in length and both sub rounded to rounded (Fig. 8A, B) and angular. The rounded samples are flat platy grains with no obvious folds or carved striated channels, while the angular grain is a bulky platy grain also with no obvious folded edges or carved striated channels. The sub rounded to rounded gold samples have grain edges that are rounded and smooth while the angular samples have a similar grain edge but also have regions on the edge that are flat and angular. The surfaces of all the samples are predominantly flat and smooth with numerous cavities, while the gold structure appears to be flat step like gold sheets which, does not contain any fine branched networks of gold. The cavities contain nano-particulate gold (Fig. 8C, D) with some of the larger cavities containing aluminosilicates and silica. These samples did not show grain boundary dissolution.

5.5 Arrowtown

Arrow Town samples are 200 – 1200 um in length, and have 3 different styles; flat and elongated (Fig 9A, B), angular with sharply defined edges and flattened rounded grains. Both the flattened elongated and rounded grains have smooth flat grain edges, which do not show any folded

edges. The angular sample also has smooth rounded edges and some sharp angular edges. Both of the flat grains, elongated and rounded, have a similar surface structure of smooth flat surface with numerous cavities protecting fragile gold forms (Fig 9E). This is made up of mostly flat step like gold sheets on the surface and branched network style of structure within the cavities. They also have some carved striations and channels on the surface due to damage. These samples show almost no inclusions of aluminosilicates or silica grains except in rare cases. One sample also contains, on the surface, a carbon based (EDAX spot analyses) long thin branching network of organic like material (Fig. 9C, D). This is isolated to one region on the gold grain about 200um2. The angular sample has a surface which is smooth and flat, with almost no cavities. It has regions of sharply defined edges and exceptionally flat surfaces that appear to cast an object which is no longer present. Rare cavities do contain branched network styles of gold which maybe dissolution features, similar to Erlebacher (2001), rather than a secondary feature. This sample has a few minor carved striated channels. Element maps across the interior of the grain show almost no change in the concentration of either gold (Fig. 9F) or silver (Fig. 9G) throughout. This is partially true based on the results of the quantification which show that; the concentration of silver on the grain rim can be a maximum of 5.68% Ag, and the grain interior has a maximum of 5.79% Ag, with an average across the grain of 5.30% Ag. Gold quantification across the grain showed a maximum concentration of 100% Au on the grain rim, with the next highest concentration of 96.89% Au. The gold concentration has a minimum concentration of 93.32% Au offset from the centre and an average across the grain of 95.81% Au. Silica was the only other detected element above detection limit with a maximum concentration of 0.16% Si within the grain, an average concentration of 0.13% Si and a detection limit of 0.06% Si. Elements below detection limit included Fe, Ni, Cu, Zn, As, Pd, Sn, Os, Ir, Pt, Hg, Pb, Al, S, Bi, and Sb, noting that these gold grains did not contain any detectable mercury, which may have an influence on gold structures.

5.6 Reefton

The Reefton samples are up to 5mm in length, with a highly texture surface consisting of at least 2 distinct styles in a nugget like (large, angular, and blocky) sample (Fig. 10A, B). The first style is rather similar to a sponge; containing a gold rich, highly textured surface consisting of many holes, pits and some inclusions of silica in a matrix like pattern of gold (Fig. 10C). Exposed surfaces have been smoothed and rounded and contain rare carved striated channels some 30um wide. The second style is silica rich matrix containing fragments of gold and gold micro-crystals (Fig. 10E). Some of the gold micro-crystals supported by the silica matrix are triangular in shape and of roughly 1um in length, while a large portion of the gold occurs as small rounded forms, no bigger than 0.5um, some having distinct angular edges (Fig 10E), as well as larger (3um) angular crystalline gold. Another texture was as observed which is neither gold nor silica supported matrix but a mix of the two (Fig.10D). This is comprised of mostly gold occurring as long thin branches (2um long by <0.5um wide) and small rounded forms (1um), along with silica.

5.7 Orepuki Beach

The Beach placer grains are between 400 - 800um in length, flat, rounded platy grains (Fig. 11A, B) and elongated, thicker grains (Fig. 11C). The flat platy grains have exceedingly thin grain edges, that are smooth and rounded while the elongated grains have thick folded edges which are also smoothed and rounded. The surface texture of the flattened grains is very smooth (Fig. 11B), but contains cavities protecting etched gold pits and nano-crystalline gold (Fig.11D, E), along with moderately developed grain boundary dissolution features in some areas (Fig. 11D). These samples do not show carved striated channels. The elongated sample grains have the same smoothed surfaced as the thin grains, but they have more deeply developed etched valleys. The valleys appear to be preferential to grain boundaries, and isolate islands of gold on the surface of the grain (Fig. 11F). A finer texture on most surfaces, except those smoothed exposed edges, is small pits on the gold surface (<100nm across) similar to the thin platy grains but much more

developed and as many as 10 per 1um. Aluminosilicate fill on the grain surface hosts many small forms of gold and fragments including nano-particulate spheroids (Fig. 11G). Element maps across the interiors of 2 grains showed one with a moderately defined silver rich core and silver depletion rim (Fig. 11M), while the other sampled displayed almost no silver in the core and a slight concentration of silver on one region of the rim (Fig. 11I). This is confirmed with the quantification showing a maximum silver concentration on the rim of one grain of 2.02% Ag, with no value recorded in the grain core despite a detection limit of 0.27% Ag. Average concentration across the grain was 0.48% Ag. Gold concentration (Fig. 11H, L) varied across the grain with a minimum of 85.37% Au recorded on one side of the grain rim, which, was not due to an increase in silver as no value was recorded here. Highest gold concentration was in the interior of the grain with a maximum of 100% Au, and an average across the grain of 93.30% Au with a detection limit of 0.28% Au. Only Silica and Aluminium were above detection limit on this grain with a maximum concentration of 3.33% Si and 0.71% Al. Silica was at the highest value on the grain rim and had an average across the grain of 0.44% Si with a detection limit of 0.05% Si. Aluminium was recorded at 2 sites within the grain interior which corresponded to the lowest gold concentration, and a detection limit of 0.06%Al. The grain with a well developed silver rich core had a maximum silver concentration of 28.61% Ag and no recorded value for silver on the grain rim despite a detection limit of 0.27% Ag. Average silver concentration across this grain was 8.23% Ag. Gold concentration was highest on this grain at the rim with a maximum of 100% Au, while the lowest gold concentration of 72.69% Au; was also the highest silver concentration in the grains interior. Average gold concentration across the grain was 91.76% Au, with a detection limit of 0.28% Au. Only silica and aluminium were above detection limit with a maximum concentration of 0.09% Si and 0.71% Al. Silica was detected on the grain rim, with a silica average across the grain of 0.02% Si, with a detection limit of 0.05% Si. Aluminium was detected in three places which coincided with the highest silver concentration; highest aluminium was 0.18% Al, with an average across the

grain of 0.05% Al and a detection limit of 0.06% Al Elements below detection limit included Fe, Ni, Cu, Zn, As, Pd, Sn, Os, Ir, Pt, Hg, Pb, Al, S, Bi, and Sb, noting that these gold grains did not contain any detectable mercury, which may have an influence on gold structures.

5.8 Echunga

The samples grains from Echunga were between 200 – 1200 um in length, blocky chunks, with smooth sub angular to rounded edges (Fig. 12A, B). The surface of these grains is smooth, containing inclusions of silica, aluminium, and rare iron oxides. The smooth surface of these grains is made up of entirely flat, step like gold sheets and do not show the small pits like the other sites, but more hollows or topographic lows in the surface and none of the surfaces show damage such as the carved striated channels. The hollows contain channels or deep valleys which appear to be between grain boundaries with 120° orientation exposing crystalline gold. One sample contained silica veins present running through the entire length of the sample (Fig. 12A, B, C), which host fine microcrystalline spheroids and triangular forms of gold no bigger than 1um (Fig. 12D).

Discussion:

Falconer (2009) summarised most of the remobilization features seen on gold grains including distinction between dissolution and precipitation features based on their morphology, silver/mercury depletion and pure gold rims. Some of the key points about identifying and determining the dissolution or precipitation characters of the features are; that dissolution acts preferentially towards surface defects and sub grain boundaries, creating first; sharply defined, sub grain boundaries developing into an overall mottled texture, in which sharply defined sub grain boundaries no longer exist and sub grain cores have been isolated. Other important features are that delicate gold forms in fluvial transport would easily be deformed and or eliminated by abrasion and that clearly defined silver depletion rims are consistent with partial leaching of silver, and also

occur on sub grain boundary rims. Depositional textures result from gold forms developing through a repeated nucleation of budlike structures to polyspheroidal aggregates or chain structures, consistent with Lengke (2007). Other fine grained gold features believed to result from precipitation include; ultrafine-grained threads or wispy veils bridging gaps between widely spaced gold spheroids and pseudo hexagonal plates described as triangular in keeping with the hexaoctahedral symmetry of gold (Bonev, 1996). Where gold precipitates via a budlike process on a large scale (tens of um's), sheets of new gold are built up in which the individual buds are commonly clearly distinguishable (Falconer, 2009), however, on the surface of polyspheroidal aggregates, the area between any two buds or gold forms is seamless, unless acted upon by dissolution. One process describing the coupled nature of gold with both dissolution and precipitation is that gold has a high electrochemical affinity for its own metal (Lawrance, 2001), whereby gold will preferentially be precipitated onto existing gold.

The Parker Road QPC grains are, from a broad area of view, grains which have been alluvially worked, showing features including the flat platy habit, folded and flattened edges, damage (i.e. carved striated channels and edge tears) and rounded thickened edges. Inclusions of silica and aluminosilicates are present and can be worked into the gold surface through the same physical action. Close surface features show a different story, with fine branched networks of gold in protected areas some covering over silica inclusions (Fig. 3C); which would have been destroyed if the inclusion was pressed into the surface by physical action, as well as broad covering across the surface of flat, step like, gold sheets; which are now interpreted as a precipitation and aggregation feature due to their similarity with Falconer (2009). Dissolution textures (Fig 3D) are present on some of the fine gold networks and step like sheets of gold while   other surfaces have no identified dissolution features. The subsurface features (Fig. 4B, C) display a region composed of microcrystalline gold on top of coarse crystalline material. Furthering on as to the aggregation of gold forms in to sheets, over time continual dissolution and precipitation would

yield a microcrystalline structure with indistinct crystalline boundaries composed of microcrystalline material that is derived from the underlying coarse crystalline gold. This is the natural phenomenon called electro refining, which is due to the fluctuating redox conditions thought to be in response to seasonal changes in drainages (water table and water flux) in which gold undergoes oxidative dissolution and reductive precipitation (Falconer, 2009; Lawrance, 2007). Concurrent with the dissolution and precipitation of the gold is the formation and breakup of nano particulate gold, which released in to the environment would further increase the reactivity towards the gold forms (Reith, 2010), or precipitation on to the nano-particulate, leading to a new gold grain over time through aggregation (Lengke, 2007). To certain extent the amount of growth or precipitation that has occurred to these grains can be interpreted as microcrystalline gold where continual dissolution and precipitation on the grains leads to both the increasing subsurface dissolution of silver and the evolution of the pure gold rim on the grain, while the process leading to silver enrichment in the subsurface (Fig 4D) is not understood.

The Gore lignite measures gold grains display many similar features to the Parker Road QPC grains. The grains display a moderate amount of damage caused by physical movement, including round, flat, platy habit, folded and thickened edges, silica inclusions, and only one grain displayed some carved striations and tears. The samples display a surprising lack of surface damage features despite the above habits caused by physical movements (Fig. 5C). The surfaces are covered by highly textured material consisting of step like gold sheets (Fig. 5C), and in cavities; fine branched networks and overgrowths. These samples display a low level of grain boundary dissolutions in select places on the surface (Fig. 5E). The features described are consistent with precipitation of gold on to the surface, covering and removing damage, creating a gold rich rim and nano-particulate formation. Using the element maps it can be seen that one grain (Fig. 5H, I) appears to have either been under extensive dissolution to remove silver from all but 2 specific locations, or has been grown from 2 nuclei containing a small amount of silver. Surface features

are indicative that these grains are currently undergoing active precipitation, leading to the idea these grains were grown from small nuclei, or nano-particulate aggregation (Lengke, 2007; Reith, 2010). Contrary to this another element map (Fig. 5F, G) displays dispersed silver throughout the interior of the grain, indicative of extensive dissolution, isolating the sub grain cores richer in silver.

Shanty Town gold is quite different with respect to the Parker Road samples, while these samples show the same effects caused by physical movement, including; flat rounded grains, folded and flattened edges, carved channels and mineral inclusions. The highly textured surface of these grains includes carbon based, long thin networks of hyphae (Watterson, 1992)(Reith, pers. comm. 2010), (Fig. 6B, C, D, E) which appear as though they are also below the surface (Fig. 6D) and are in close proximity to vast regions of nano-particulate gold (Fig. 6C). This causes speculation as to whether the hyphae may interact with the gold in such a way that promotes the formation of these nano-particulates. These samples have the same gold structures seen on the Parker Road samples including flat, step like, gold sheets covering the surface and branched gold networks in protected cavities indicative of active precipitation, while some areas have highly developed grain boundary dissolution, in some cases isolating individual gold sub grain cores. These grains are highly electrorefined with an average gold concentration (Fig. 6G) of 99.44%, with very low silver recorded in the grains interior, also leading to the idea that these grains may have aggregated from nano-particulates, which are now being actively produced and likely dispersed, or have had extensive dissolution-reprecipitation events, growing the grains. The subsurface of the grains is similar to the Parker Road samples, with microcrystalline and coarse crystalline gold, but more detail shows free microcrysts in the polymorphic layer retain crystalline orientations (Fig. 7E), and another feature not seen in the Parker Road samples are long thin bands in the microcrystalline subsurface which resemble a mylonitic structure (Fig. 7D). Mentioned previously repeated dissolution – reprecipitation events are likely to produce a subsurface

composed of microcrystalline gold with indistinct crystalline boundaries and orientations (Fig. 7B, C, D). This is observed to the full depth of the section viewed (Fig. 7A), but interestingly, coarse crystalline gold occurs only at the top of the section (Fig. 7B). Another feature similar to Parker Road is a deep subsurface polymorphic region, with very similar features to the current surface covering (Fig. 7A). Interpreting this gold grain as having grown by repeated dissolution and reprecipitation events, it is likely this is a remnant surface which has been completely covered by precipitating gold, or that this gold has experienced a refolding event; which would likely yield a surface composed of coarse crystalline gold, richer in silver since it would contain part of the grain interior.

The samples from Kawarau gorge contain grains with a fluvial habit; rounded, flat, platy grains (Fig. 8B), but also have samples which are of a much more blocky nature, with sharp angular edges. These grains show both flat, step like gold sheets (Fig. 8C) and nano-particulate gold within protected cavities (Fig. 8D), but no recognisable dissolution features. These grains have gold precipitation features (i.e. step like gold sheets resulting from aggregation), and nano-particulate formation, the dispersion of nano-particulates could provide a source of gold for later aggregation or precipitation on to other similar gold grains.

Arrow Town sample grains show the same typical fluvial transport features as with previous samples; flat rounded grains, smooth surface with flat, step like, gold sheets, branched network and fragile gold forms (Fig. 9E) within protected settings. They also show carved channels with striations indicative of fluvial damage. Other non typical features include one sample grain showing a carbon based hyphae structure on the surface, and one sample grain of a blocky nature with angular edges, smooth flat surface and rare cavities. This sample has a region on it which appears sharply defined as if it is casting an object which is no longer present. An unusual feature of this sample set is that they contain almost no inclusions of silica or aluminosilicates. These grains have very little development by way of silver dissolution in the grain interiors, but do show

a pure gold rim (Fig. 9F). The high silver concentration in the interior and with very little change in the rim by way of silver dissolution, leads to the idea that these grains are derived by weathering of a host containing the gold, with little post weathering to remove silver, but have had active gold precipitation on the surface for the development of the gold rim and secondary structures (Fig. 9E). The blocky grain showing the cast is likely an original structure still present, of the host body containing this gold, as this grain shows dissolution pits primarily instead of the precipitation features seen on the other samples. The differences in the sample morphology may also be due to two different gold sources both providing samples to this site which have experienced different conditions; one leading to active reductive precipitation and the other a very mild oxidative dissolution condition, since silver rim dissolution has very little development.

The Reefton samples show a highly developed dissolution surface morphology, referred to as appearing like a sponge. The surface contains many dissolution pits and is gold rich, likely due to silver dissolution, and contains carved striated channels indicative of damage. This gold also contains a silica matrix rich in gold fragments and small triangular gold forms strikingly similar to Falconer's (2009) pseudo hexagonal / octahedral gold platelets, as well as small rounded gold particulates and some with distinct angular edges. Long thin gold branches are identified which also resemble the polyspheroidal aggregates in Falconer (2009) as chain aggregated budding style structure. These grains have likely been formed in a silica vein hosted system, in which gold platelets reflect either rapid precipitation of gold from a supersaturated solution (Lawrance, 2007), or have aggregated from nano-particulates during formation (Southam, 1994; Southam, 1996). It is noted that the secondary gold formation for these grains, happened during the formation of the vein hosted system, and not post weathering as seen in the other systems. Post gold release from the silica vein system has resulted in only dissolution and fluvial damage effects being active on exposed gold surfaces with no secondary precipitation.

The beach placer grains display a highly developed fluvial habit; of exceeding thin, flat, rounded, platy grains (Fig. 11B) and elongated flat grains with thickened edges (Fig. 11C). The surface is pocket-marked with etched dissolution pits (Fig. 11D), and highly developed grain boundary dissolution features in moderately protected settings (Fig. 11F). Nano-particulate gold is present within a number of etched pits (Fig. 11D, E), and is likely released due to the etching and dissolution effects recorded by the surface features. The extensive dissolution and etch features on these grains may portray the effect that salt water may have on the morphology of these grains. Element maps of some grains show almost complete removal of silver from the grains, including the interior (Fig. 11I), while some still have small regions richer in silver (Fig. 11M). The removal of silver and extensive dissolution features on the surfaces support the possibility which salt water may have on the morphology of these grains.

The Echunga samples display a blocky habit, not displaying any damage features typical of fluvial movements, despite being collected from a paleochannel system. The surfaces show no damage, and very little rounding, while some of the exposed edges are still quite angular. These grains contain inclusions of silica, alumina and rare iron oxides, and the surface consists of flat, step like, gold sheets reminiscent of gold precipitation. Only 1 select area on a grain contained a feature of advanced grain boundary dissolution, exposing the 120° crystalline habit of the gold, despite not occurring on any other surfaces. The possibility exists of a false interpretation as to grain boundary dissolution, under an electron backscatter response, or whether this is just undamaged crystalline gold exposed on the surface, under secondary electron imaging, with sharp 120° angles. Two of the sampled grains showed regions of silica as part of the gold grain, with one sample having veins running through the gold (Fig. 12A). These veins (Fig. 11C) contained both nano-crystalline and small triangular, pseudo hexagonal / octahedral gold platelets (Fig. 11D). These grains may have formed under a similar process to the Reefton samples in which secondary gold formation happened during the formation of the silica hosting body. The Echunga grains post

weathering and fluvial transport, display gold precipitation; cleaning and removing any damaged features on the surfaces. Of note is that these are Tertiary river gravels currently containing the gold, which are most likely older and more developed than those of the grains of New Zealand's goldfields.

The influence which different environments have on gold morphologies is quite dramatic; from the saltwater etched samples of the beach placer, with extensive dissolution features, to the fluvial habit of Parker Road (QPC and Gore lignite measures), Shanty Town, Kawarau gorge, and Arrowtown, with coupled dissolution and precipitation features, to the silica vein hosted samples of Arrow Town, Reefton, displaying predominantly dissolution features and Echunga which displays precipitation features. One thing which all the sample sites share, no matter whether dissolution or precipitation is the dominant effect, is that of the presence and production of nano-particulate gold forms. These are generally small (<0.5um) spheroids, occurring in clusters within protected cavities or etched pits in the grains surface. Subsurface images display the ability of the small spheroids within a polymorphic surface layer to retain crystalline orientations, and the etching of underlying gold to form these. It is likely that gold nano-particulates that have been released from the gold surface have either undergone chemical mobilization, resulting in precipitation, or aggregation onto other gold grains or nano-particulates, leading to a growth of the host grain with a microcrystalline subsurface makeup, or a larger environment gold halo, such as calcrete anomalies.

The structures and features observed on the gold grains sampled are features which can be applied to just about anywhere, as they are features resulting from the influence of the supergene environment. The use of New Zealand gold in this study is because New Zealand has highly active systems and processes, and subsequently the gold also displays this with the structures observed being particularly pronounced. The activity of the gold systems and the surrounding environment has a direct influence on the secondary gold structures created or destroyed, particularly gold nano-

particles. Gold nano-particulates are created through the recycling of underlying gold (Reith, 2010) as observed in Fig. 7A, since the available gold complexes in solution is often very minute, while the underlying gold presents an abundance of source material. It is therefore assumed areas with low activity or processes would have faint or difficult to recognise structures due to the long time it would take for the processes, i.e. precipitation of new gold, and the likelihood of other effects leading to the breakup or damage of any features.

Conclusion:

Its is observed that gold grains sampled from a range of New Zealand's environment consist of gold of either a fluvial or silica vein style habit, with or without fluvial caused damage, contain a range of precipitation and dissolution features. Precipitation or dissolution may be the dominant feature, and all sites sampled contain gold as nano-particulates which are being actively produced. Release of gold nano-particles from a parent grain can result in a great environmental mobility of gold and later aggregation or precipitation; most likely onto pre-existing gold particles which results in the growth of gold grains in the supergene environment. The continual dissolution and precipitation, through fluctuating redox conditions can result in a subsurface makeup of microcrystalline gold with indistinct crystalline boundaries and non-linear crystalline orientations, with a polymorphic layer producing nano-particulates and precipitating secondary gold forms. Hyphae have been seen in close proximity to large regions of gold nano-particulates and may influence the production of nano-particulates from underlying gold.

References:

Bonev, I.K., and Vesselinov, I. (1996) Comments on the paper by L.M. Lawrance and B.J. Griffin. Mineralium Deposita, 31, 348-349.

Craw, D., Norris, R.J. (1991) Metamorphogenic Au-W veins and regional tectonics: mineralisation throughout the uplift history of the Haast Schist, New Zealand. New Zealand Journal of Geology and Geophysics, 34, 373-383.

Erlebacher, J., Aziz, M.J., Karma, A., Dimitrov, N., Sieradzki, K. (2001) Evolution of Nanoporosity in Dealloying. Nature, 410, 450-460.

Falconer, D.M. (2003) Sediment hosted gold and sulphide mineralisation, Belle-Brook, Southland, New Zealand. Unpublished M.Sc. Thesis. University of Otago, 373.

Falconer, D.M., Craw, D., Youngson, J.H., and Faure, K. (2006) Gold and sulphide minerals in tertiary quartz pebble conglomerate gold placers, Southland, New Zealand. Ore Geology Reviews, 28(4), 525-545.

Falconer, D.M., Craw, D. (2009) Supergene Gold Mobility; A Textural and Geochemical Study from Gold Placers in Southern New Zealand. Society of Economic Geologists, 14, 77-93.

Hough, R.M., Butt, A. R. M., Reddy, S. M., Verrall, M. (2007) Gold nuggets: supergene or hypogene. Australian Journal of Earth Sciences, 54, 959-964.

Isaac, M.J., Lindqvist, J.K. (1990) Geology and lignite resources the East Southland Group, New Zealand. New Zealand Geological Survey Bulletin, 101.

Koons, P.O., Craw, D. (1990) Gold mineralisation as a consequence of continental collision: an example from the Southern Alps, New Zealand. Earth and Planetary Science Letters, 103, 1-9.

Lawrance, L.M. (2001) Mulit-element dispersion within salt lake environments: Case study of the buried Hannon South gold deposit, Western Australia. Geochemistry, Exploration, Environment, Analysis, 1, 323-339.

-. (2007) The supergene behaviour of gold: A natural enrichment and refinement phenomenon: Proceedings of Advances in understanding of supergene processes. Ores and Oregenesis symposium, Tueson, Arizona, 9-10.

Lengke, M.F., Fleet, M. E., Southam, G. (2006b) Morphology of gold nanoparticles synthesized by filamentous cyanobacteria from gold(1)-thiosulfate and gold(III)-chloride complexes. Langmuir, 22, 2780-2787.

Lengke, M.F., Ravel, B., Fleet, M. E., Wanger, G., Southam, G. (2006a) Mechanisms of gold bioaccumulation by filamentous cyanobacteria from gold(III)-chloride complexe. Environmental Science and Technology, 40, 6304-6309.

Lengke, M.F., Southam, G. (2005) The effect of thiosulfate-oxidising bacteria on the stability of the gold-thiosulfate complex. Geochim. Cosmochim., 69, 3759-3772.

-. (2007) The Deposition of Elemental Gold from Gold(1)-Thiosulfate Complexes Mediated by Sulfate-Reducing Bacterial Conditions. Society of Economic Geologists, Inc., 102, 109-126.

McCann, R., Craw, D. (2009) Gold and Platinum Deformation, Aeolian deformation and Teroid Development in Beach placer deposits, Southland. AusIMM New Zealand Branch Conference, 1-13.

Morteani, G. (1999) Gold: Progress in Chemistry, Biochemistry and Technology. Wiley and Sons: Chichester, UK, Chapter 2.

Mossman, D.J., Reimer, T., Durstling, H. (1999) Microbial processes in gold migration and deposition: modern analogues to ancient deposits. Geosci. Can., 26, 131-140.

Reith, F., Fairbrother, L., Nolze, G., Wilhelmi, O., Clode, P., Gregg, A., Parsons, J. E., Wakelin, S., Pring, A., Hough, R., Brugger, J. (2010) Nanoparticle Factories: Biofilms hold the Key to Gold Dispersion and Nugget Formation. Publication pending, 1-24.

Reith, F., Lengke, M. F., Falconer, D., Craw, D., Southam, G. (2007) Winogradsky Review: The geomicrobiology of gold. International Society for Microbial Ecology, 1-18.

Southam, G., Beveridge, T. J. (1994) The in vitro formation of placer gold by bacteria. Geochim. Cosmochim., 58, 4227-4230.

-. (1996) The occurence of sulfur and phosphorus within bacterially derived crystalline and pseudocrystalline gold formed in vitro. Geochim. Cosmochim., 60, 4369-4376.

Watterson, J.R. (1992) Preliminary evidence for the involvment of budding bacteria in the origin of Alaskan placer gold. Geology, 20, 315-318.

Figure Captions

Figure 1   New Zealand sample site locations; (a) Parker Road site, WSW of Gore, (b) Kawarau George, west of Cromwell; Central Otago sample site, (c) Shanty Town (yellow arrow), south of Greymouth, and Reefton (red star), (d) Orepuki beach, west of Invercargill, (e) Echunga, South Australia

Figure 2   Secondary electron micrographs of the Shanty Town gold grains showing the method of using the Fib; (a) site selection, with specific criteria to optimise the result and local electro - platinum deposition over the area to be Fib milled with a current of 2pA/um2, (b) Initial high current Fib milling at 30KeV and 21nA,(c) final cleanup low current Fib milling at 30KeV and 0.21nA to display below surface grain features, (d) finished Fib milled face ready for analysis

Figure 3   Secondary electron micrographs of gold grains from the Parker Road QPC; (a) typical size and morphologies, (b) intermediate surface image displaying pits and scratches, (c) gold overgrowths on silica inclusions and grain boundary dissolution, (d) various stages of grain boundary dissolutions. (e) Micrograph of polished section and quantitative electron microprobe analyses of Au (max. conc. 100 ± 0.27wt. %) and Ag (f) (max. conc. 11.12 ± 0.26wt. %)

Figure 4   Secondary electron micrographs of the Parker Road QPC gold grains of (a) Fib analyses site prior to cutting, (b) platinum coat and initial cut made using Fib displaying gold silica surface layer, (c) cut 'n' slice analyses site displaying gold silica surface layer, lower microcrystalline gold structure, and a lower gold silica inclusion, (d) electron dispersive x-ray analyses of C showing a band of higher Ag conc. in the microcrystalline gold, relative to the surface or lower layers.

Figure 5   Optical micrograph (a) and secondary electron micrograph (b) showing typical size of morphology of Gore lignite measures gold grains, (c) intermediate surface image showing smooth surface and textured pits, (d) nano-particulate gold within a pit, (e) grain boundary dissolutions and overgrowths of a silica inclusion. Micrograph of polished section and quantitative electron microprobe analyses of Au (f; max. conc. 100 ± 0.27 wt. % and h; max. conc. 100 ± 0.27 wt. %) and Ag (g [equivalent to f]; 3.17 ± 0.26 wt. % and (i [equivalent to h]; 8.57 ± 0.26 wt. %)

Figure 6   Secondary electron micrographs of (a) typical size and morphology of Shanty Town grains, (b) intermediate surface image displaying long smooth interconnected root like structure of possibly hyphae, (c) back scatter electron micrograph of gold nano-particulates, surface pits and hyphae, (d) secondary electron micrograph of hyphae and surface pit, (e) back scatter electron micrograph of the same location as d, displaying gold nano-particulates, (f) secondary electron micrograph of nano-

particulates and bud like structures in a silica rich, pit.Micrograph of polished section and quantitative electron microprobe analyses of Au (g; max. conc. 100 ± 0.28 wt. %), Ag (h; max conc. 36.7 ± 0.27 wt. %) and Fe (i; max conc. below detection limit)

Figure 7   Secondary electron micrographs of a Fib milled section (a), showing crystal orientations, (b) showing the relationship of crystalline and microcrystalline gold and sub-horizontal layering, (c) overview of polymorphic layer and underlying microcrystalline gold, (d) fine sub vertical banding and microcrystalline gold, and (e) crystal orientation of fine microcrysts of gold within the polymorphic layer.

Figure 8   Optical (a) and secondary electron micrographs (b) showing typical size and morphology of the Central Otago gold grains, (c) intermediate surface image displaying smooth grain surface and a pit (d) containing nano-particulate gold

Figure 9   Optical (a) and scanning electron micrograph (b), showing the typical size and morphology of the Arrow Town gold grains, an intermediate surface image (c) showing hyphae like structures, smooth surface and many pits, (d) a back scatter electron micrograph of the same location as c, showing silica inclusions and dark hyphae like patterns, (e) secondary electron micrograph showing bud like structures protected within a surface pit.Micrograph of polished section and quantitative electron microprobe analyses of Au (f; max. conc. 100 ± 0.28 wt. %), Ag (g; max. conc. 5.87 ± 0.27 wt. %) and Fe (h; max. conc. below detection limit).

Figure 10   Optical micrographs (a) and back scatter electron micrographs, displaying typical size and morphology of the Reefton gold grains, (b) intermediate surface structure displaying etched gold highs and silica/gold rich valley fills, (c) intermediate image displaying etched surface features, (d) gold/silica fill and (e) nano-particulate and triangular (octahedral) gold micro crystals

Figure 11   Optical micrograph (a), secondary electron micrograph (b), and back scatter electron micrographs displaying typical size and morphologies (a, b and c) of Orepuki, Beach placer grains. Intermediate surface image (d) displays a broad view of gold nano-particulates (e), (f) a broad intermediate surface image of the same grain as c and the effect of saltation weathering on the gold grain surface, and (g) nano-particulates in a silica/gold fill and saltation weathering on gold grain f. Micrograph of polished section and quantitative electron microprobe analyses of Au (h and l respectively; max. conc. 100 ± 0.28 wt. % and 100 ± 0.28 wt. %), Ag (i and m respectively; max. conc. 2.02 ± 0.27 wt. % and 28.61 ± 0.27wt. %), and of Fe(j and n respectively; max. conc. below detection limit)

Figure 12   Optical micrograph (b) and back scatter electron micrographs of the Echunga, Australia gold grains displaying typical size and morphology (a), intermediate surface image (c) displaying silica/gold veins within the gold grain and (d) displaying nano-particulate and triangular (octahedral) gold crystals present within the silica/gold veins.

Figure 1
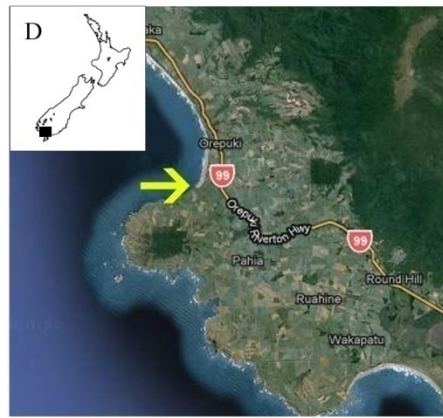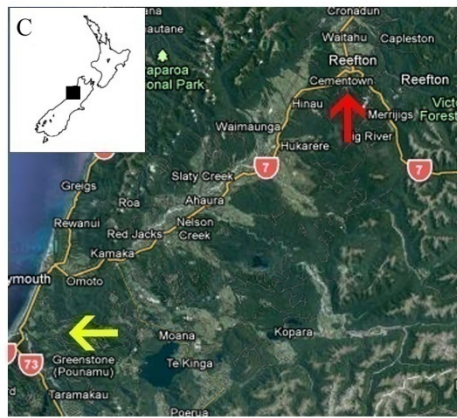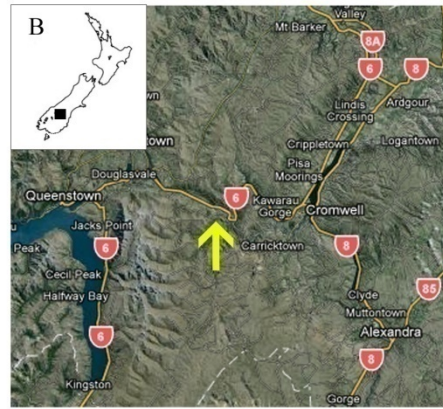
Figure 2
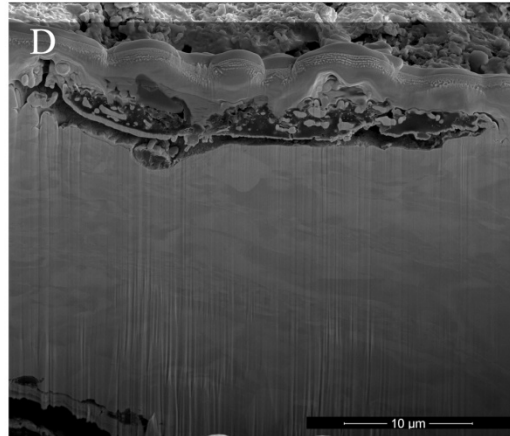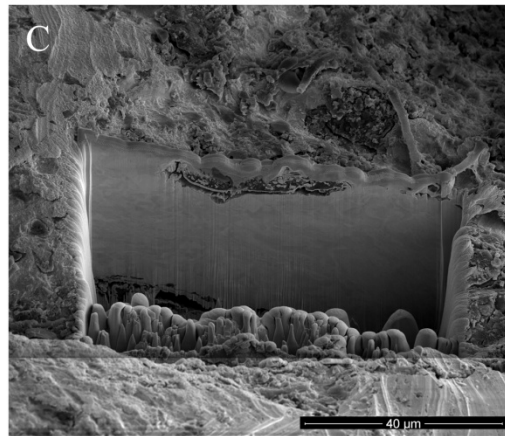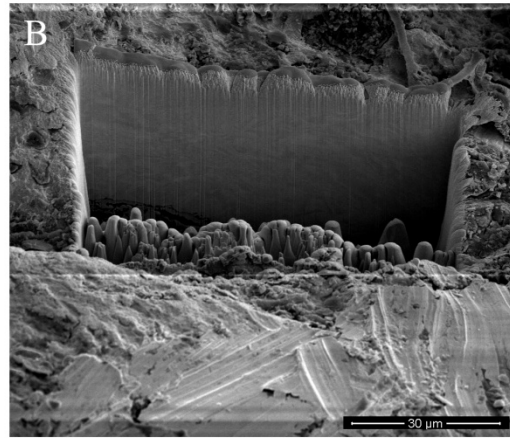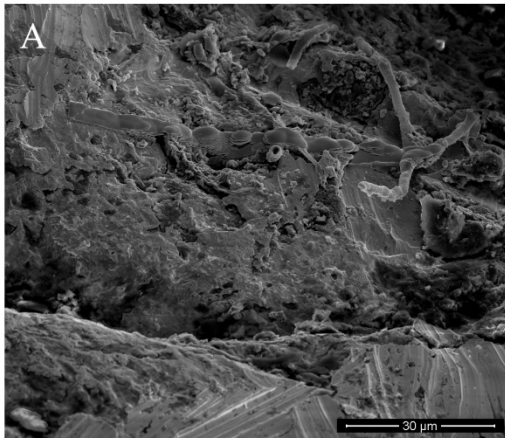
Figure 3

Figure 4

Figure 5

A

200 μm

B

200 μm

F

Au

G

Ag

H

Au

I

Ag

Min   Max

C

5 μm

D

5 μm

1 μm

E

41
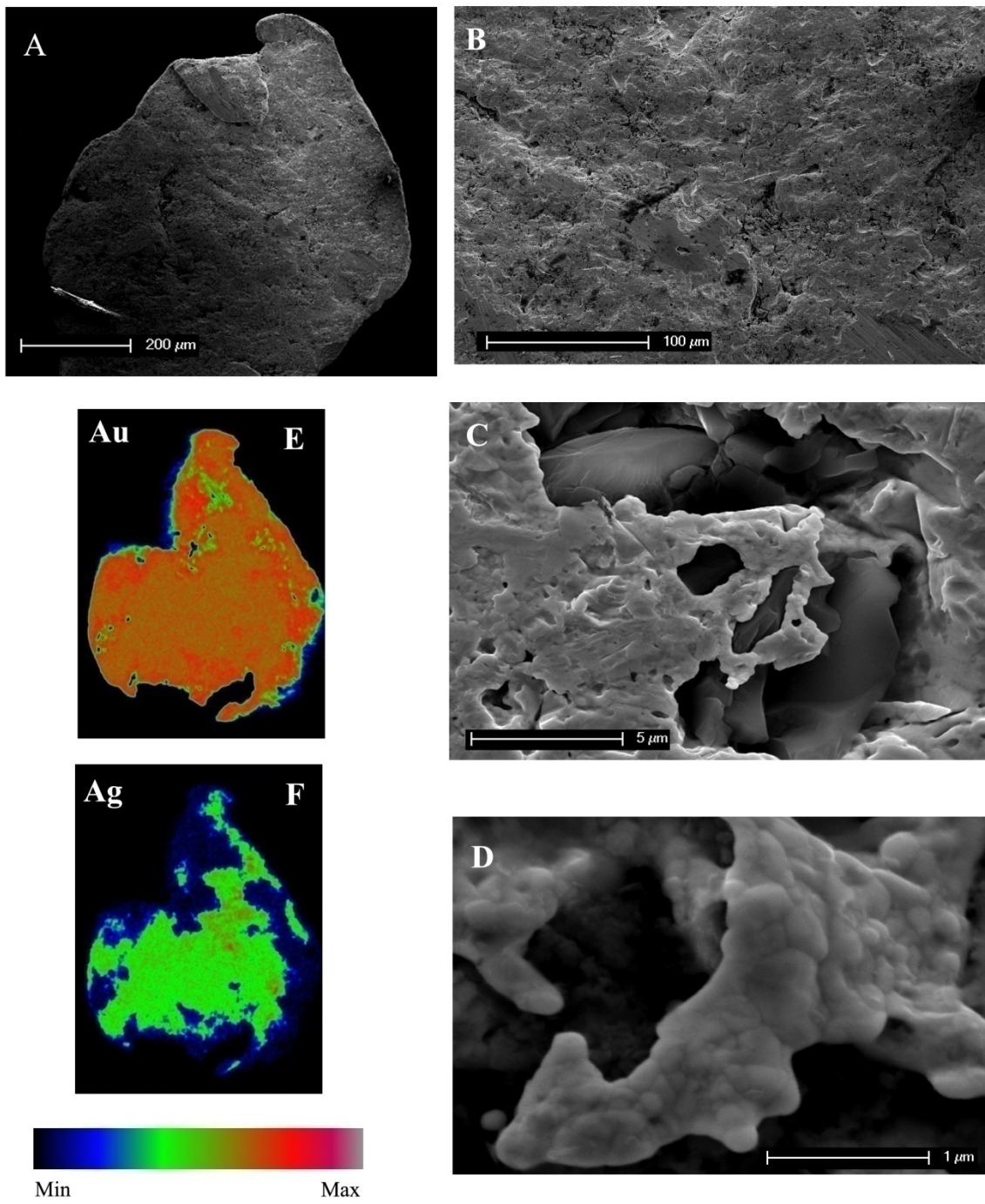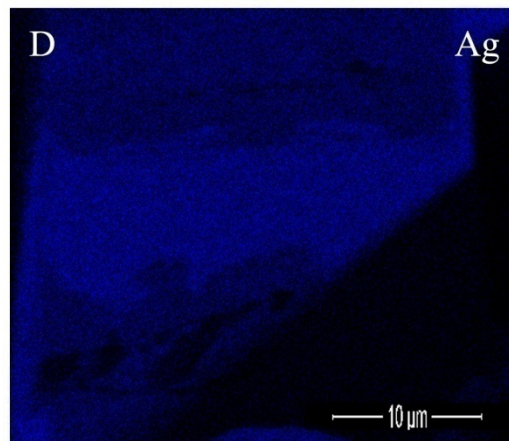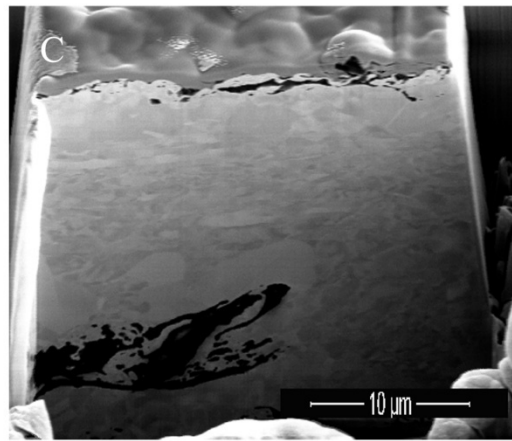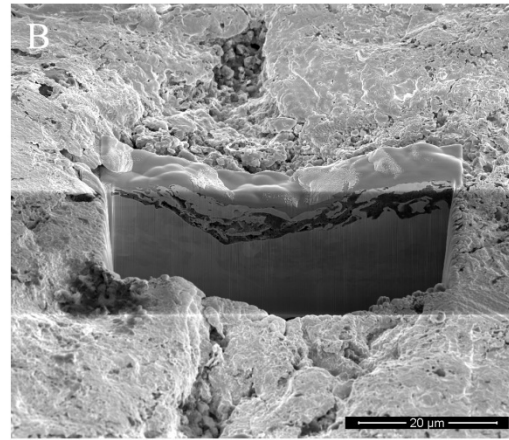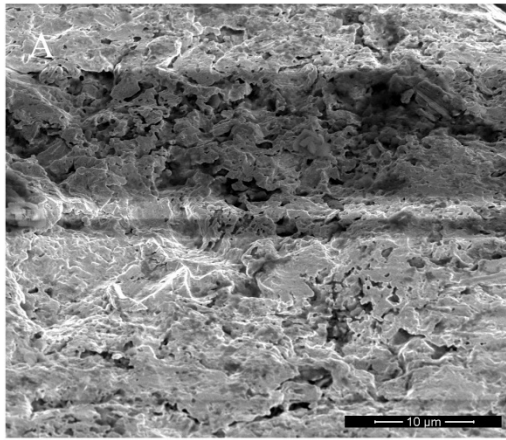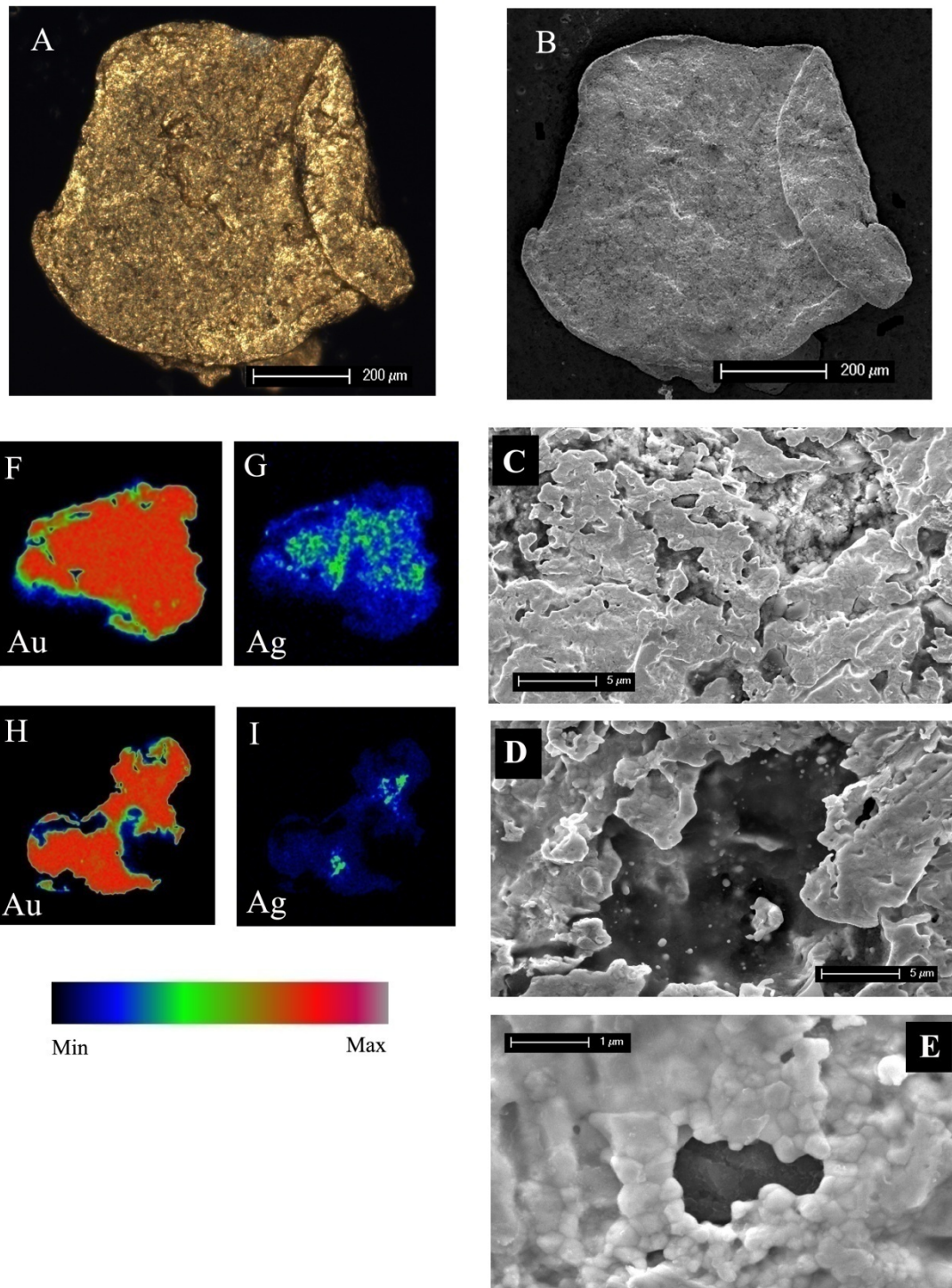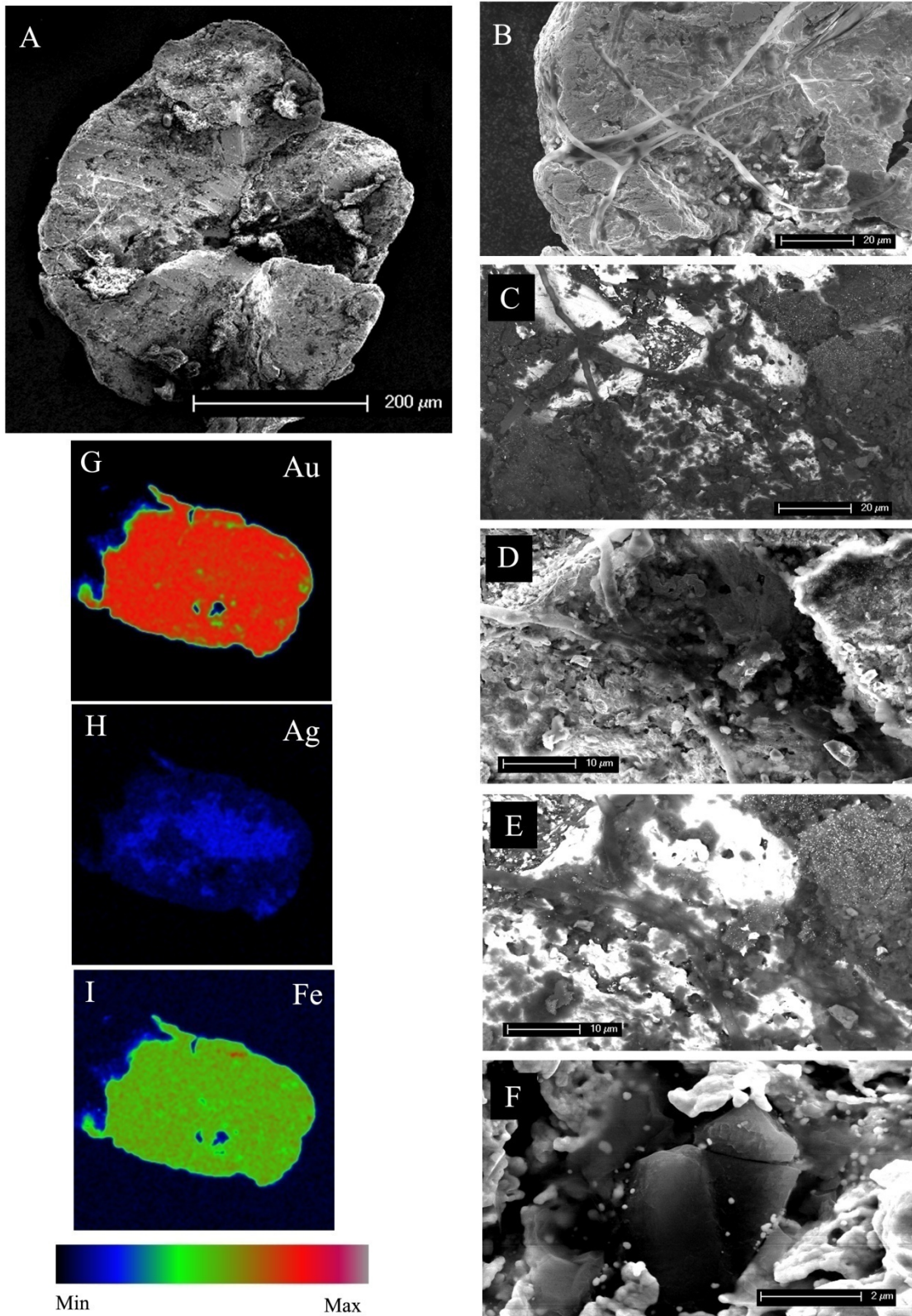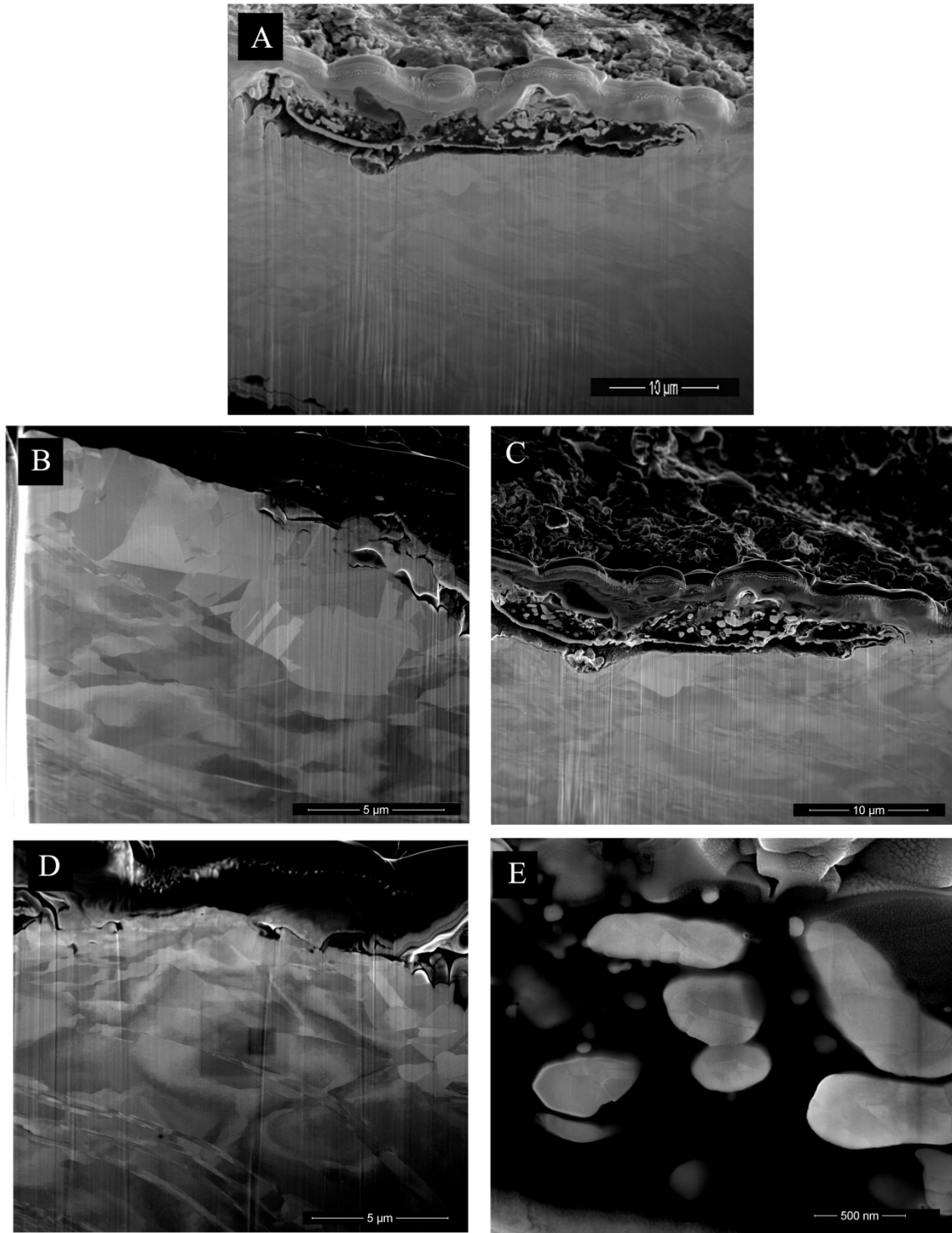
Figure 6

Figure 7

Figure 8
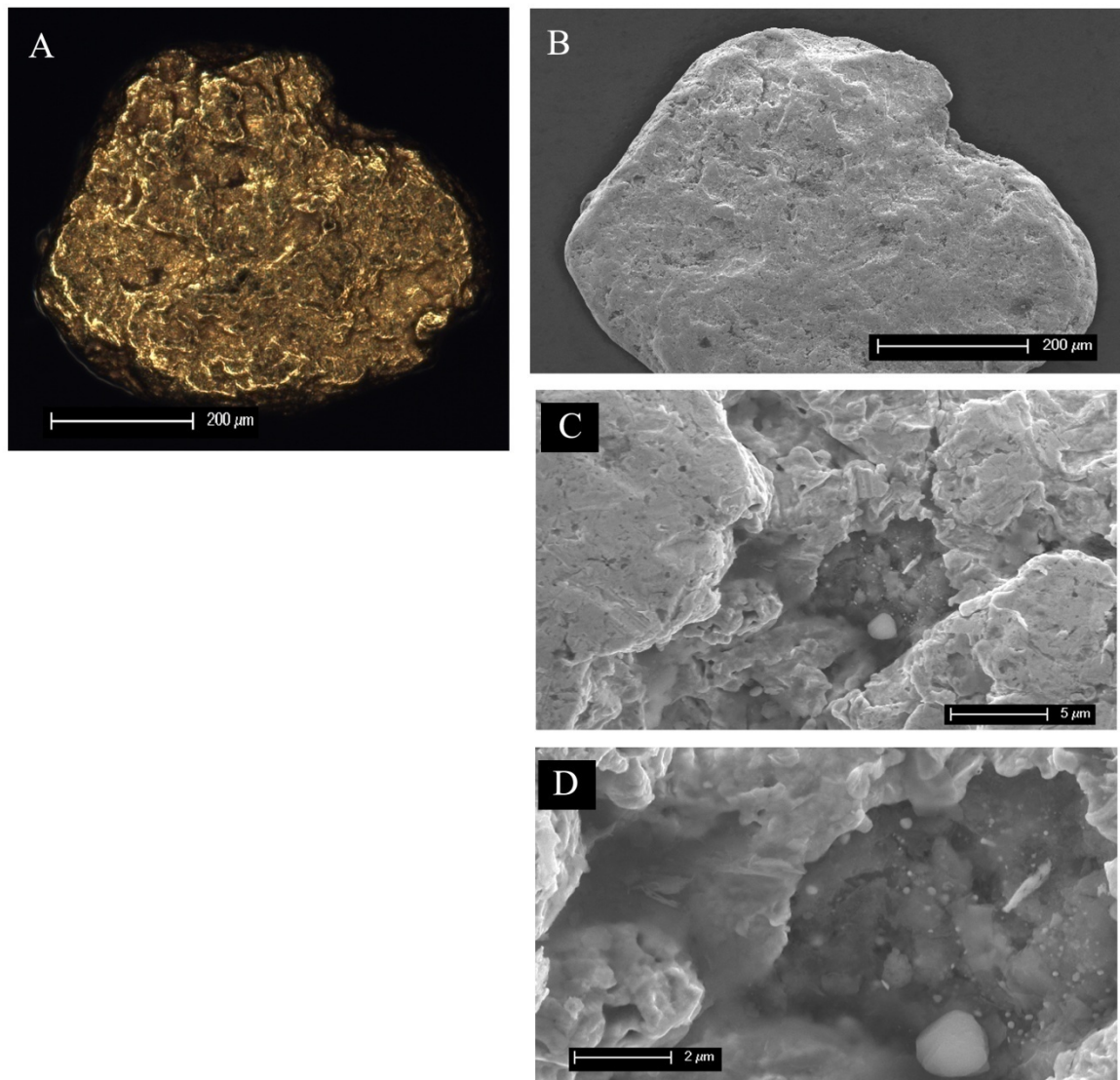
Figure 9

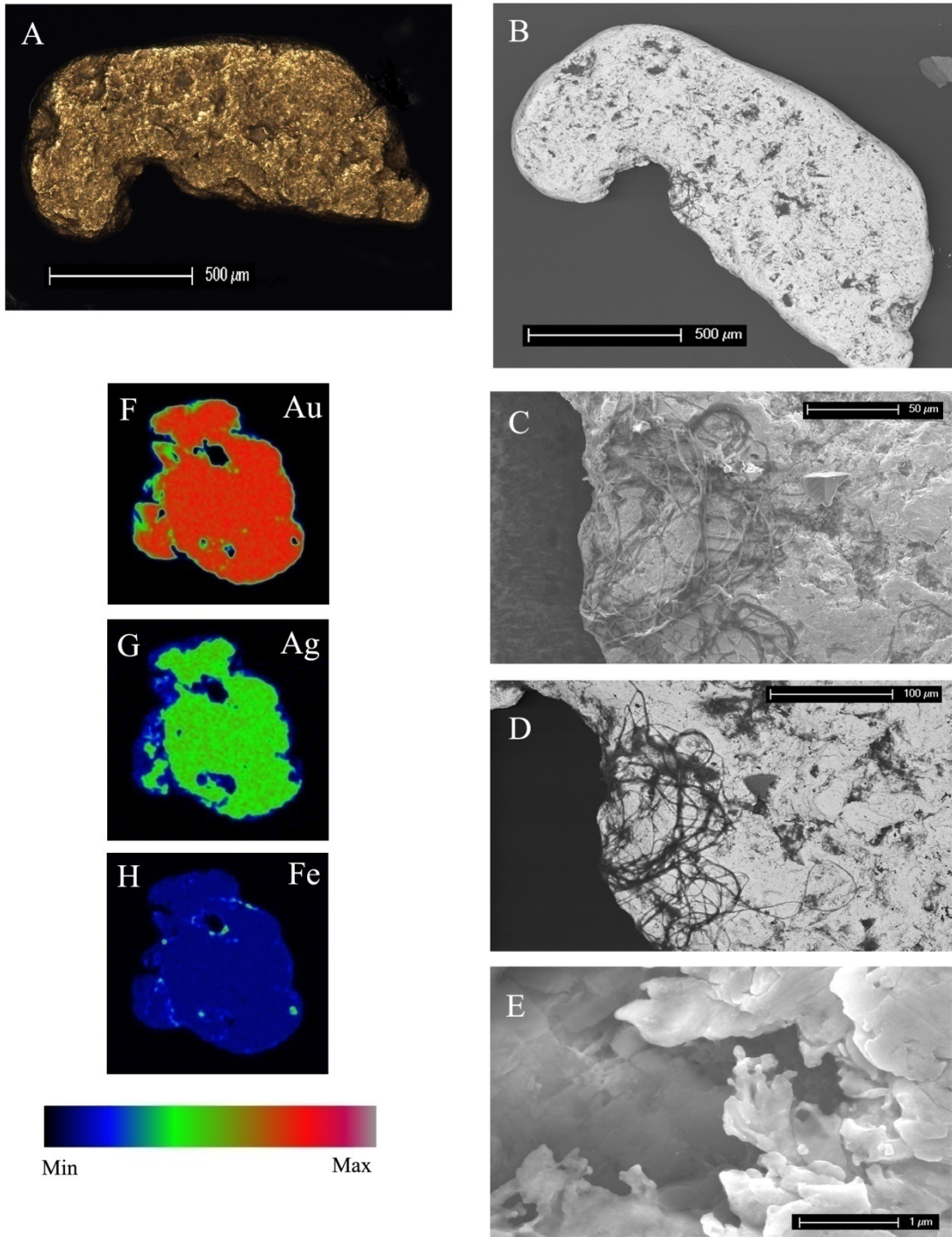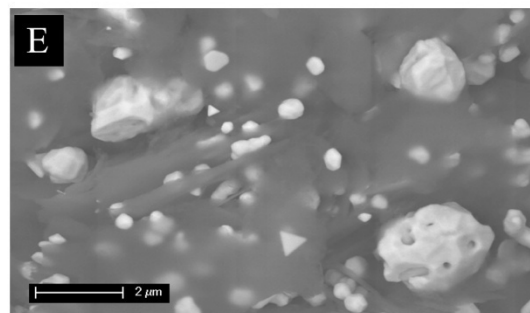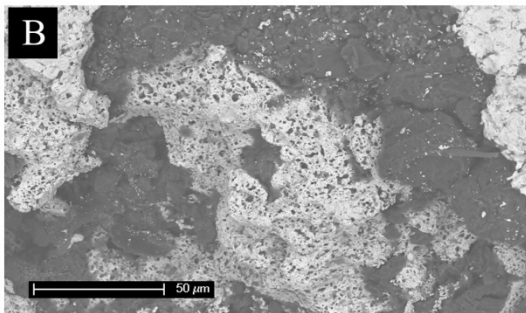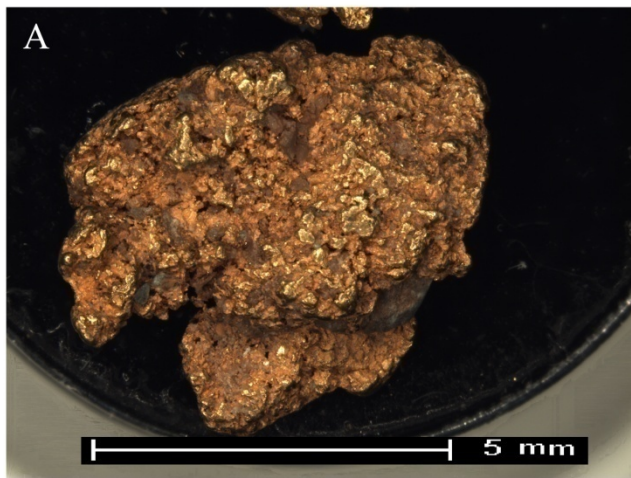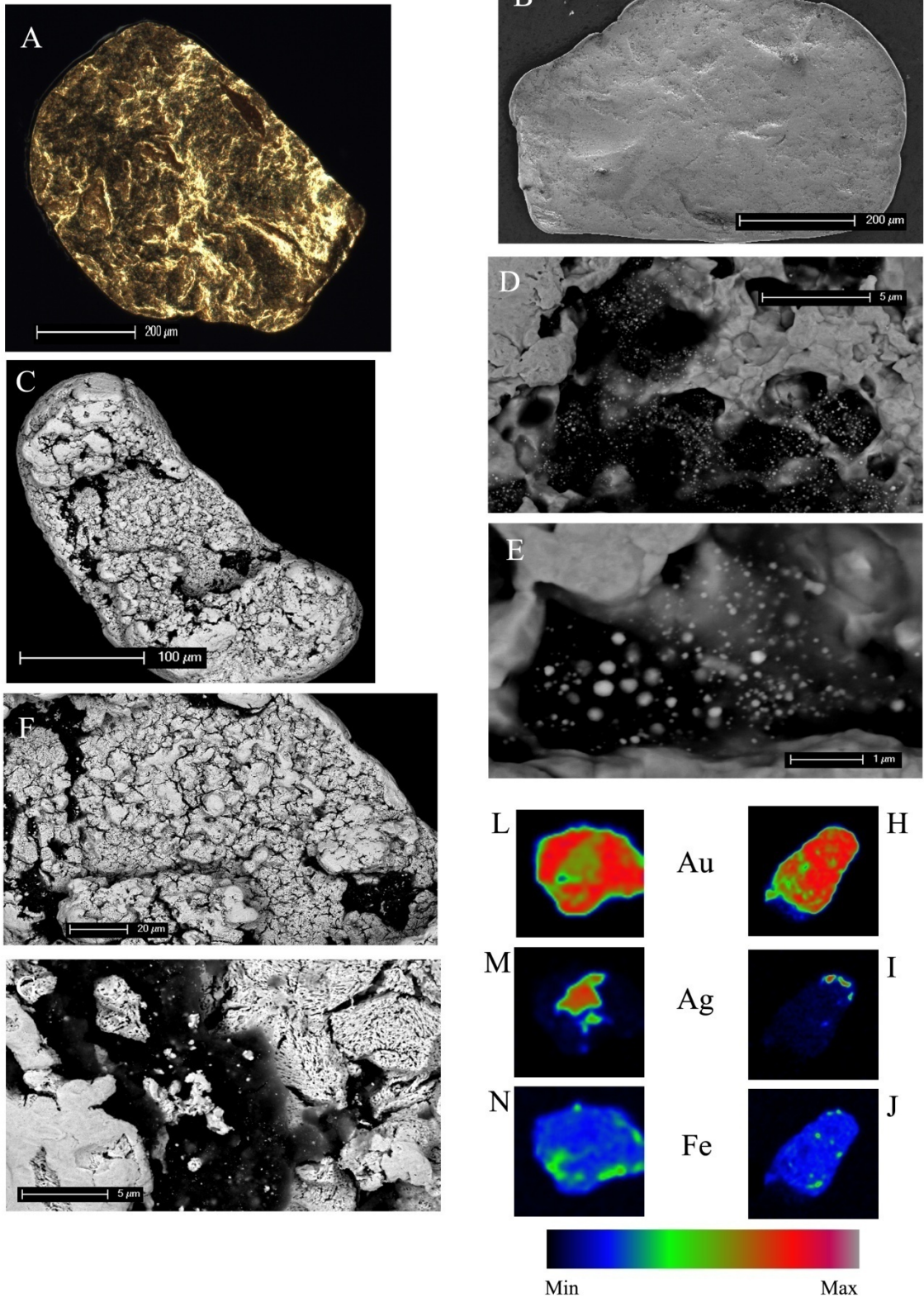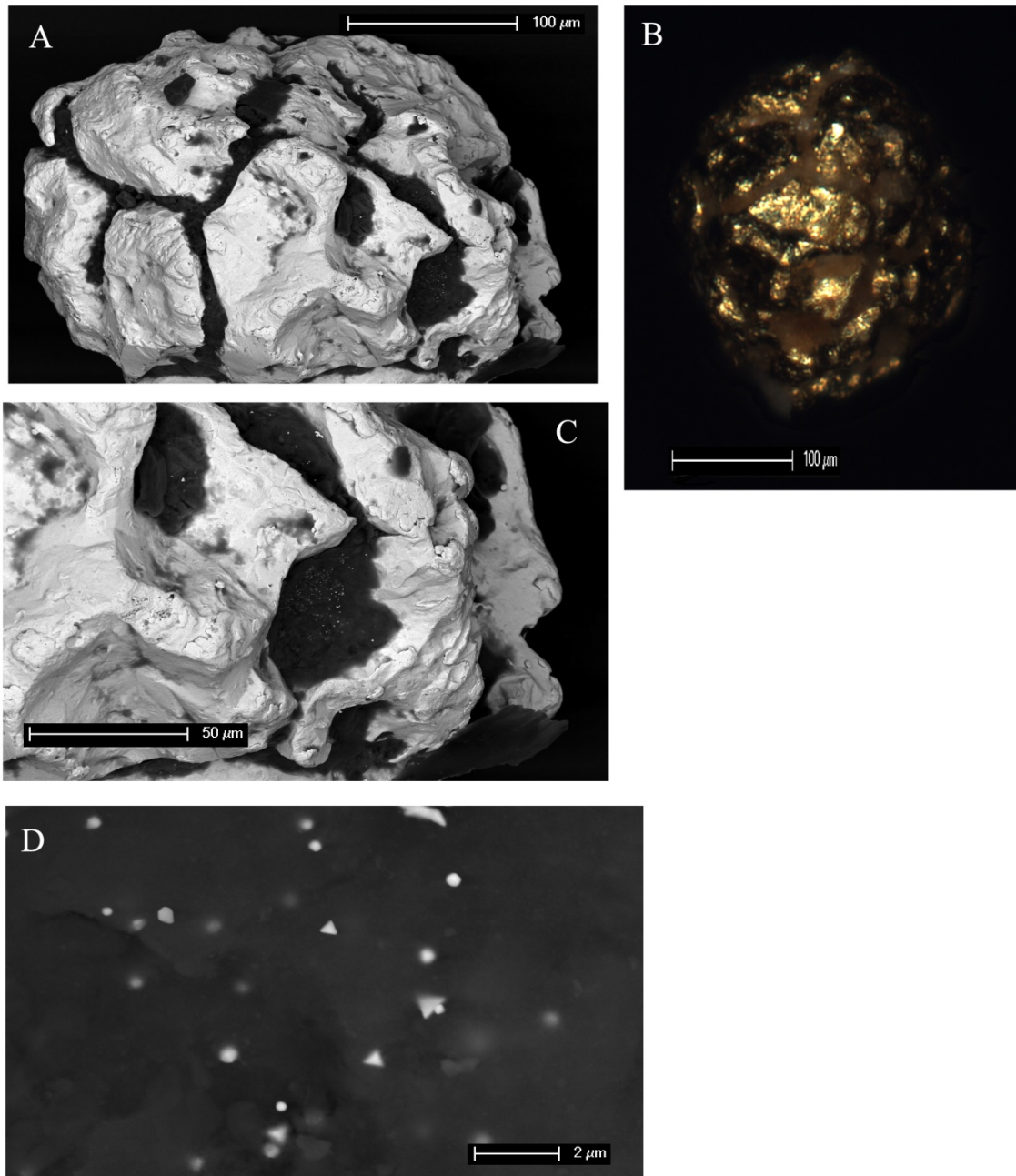Figure 10
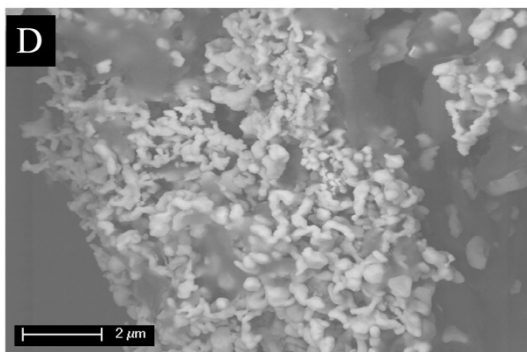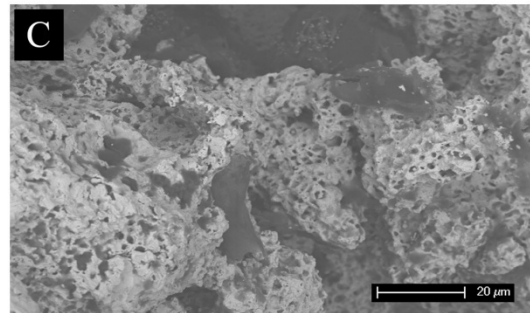
Figure 11

Figure 12

Supplementary Figures:

Figure S1   Site photos from Parker Road site; displaying (a) QPC gravels and (b) Gore lignite measures, (c) Shanty Town, (d) Kawarau gorge, (e) Arrowtown, (f) Orepuki beach place

Figure S2   Movie file consisting of 116 individual frames representing 5um thick slices, of a Fib milled region. This movie shows abundant void spaces in the top layer of the gold grain, as well as a complex cavity below a band of microcrystalline gold and a region of large crystalline gold.

Figure S1